Optimal Integral Sliding Mode Controller Design for Micro Gyroscope Based on Time Delay Estimation

Mohammad A. Faraj [1*], Sameh Jassam [2], Ahmed K. Abbas [3]
[1, 2] College of Engineering, Electrical Engineering Department, University of Anbar, Ramadi, Iraq
[3] Department of Construction and Projects, University Headquarter, University of Anbar, Ramadi, Iraq
Email: [1] Mohammed.Faraj@uoanbar.edu.iq, [2] samehjassam@uoanbar.edu.iq, [3] ahmed89at@uoanbar.edu.iq
*Corresponding Author

***Abstract*—Controlling Micro-Electro-Mechanical Systems (MEMS) gyroscopes often involves dealing with uncertainties and external disturbances, which can complicate control strategies. This article proposes a novel control strategy that integrates Integral Sliding Mode Control (ISMC) with Time Delay Estimation (TDE) and Arithmetic Optimization Algorithm (AOA) to enhance control performance. The proposed controller, OTDISMC, is designed to eliminate chattering and improve robustness against disturbances without relying on system dynamics. Contrary to the conventional controllers structures which depended on the system dynamic in their schemes, a model free controller is formulated without using system dynamics in its formulation. Time delay estimation technique has been undertaken as an efficient approximating strategy to approximate and compensate the lumped uncertain dynamics of the system. AOA has been undertaken to determine the optimum solutions of the coefficients of proposed control approach. The stability has been analyzed and investigated using the Lyapunov stability criterion. To show the effectiveness and validity of the developed controller, computer simulations in nominal and robustness scenarios have been carried out and compared with TDISMC that tuned by trial and error and PSO-TDISMC that tuned by particle swarm optimization (PSO). Simulation results demonstrate that OTDISMC significantly reduces tracking errors and improves robustness. The results indicate the superiority of the proposed controller as compared with traditional TDISMC tuned by classical methods and PSO-TDISMC tuned by particle swarm optimization (PSO).**

Keywords*—MEMS Gyroscope; Sliding Mode Control; Arithmetic Optimization Algorithms; Time Delay Control; Model Free Controllers.

I. INTRODUCTION

Recently, Micro gyroscopes has been considered as one of the most well-known devices that are used in measurement technology. MEMS gyroscopes is the core element of inertial navigation system. MEMS gyroscopes normally used in measurement process of angular velocity of different devices. Due to its unique properties represented by compact size, suitable price, low power consumption, MEMS gyroscopes have been undertaken as an efficient angular velocity instrument in wide range of applications such as: aviation, aerospace, automobiles, smart robotics, military, marine and bioengineering [1]-[2].

MEMS gyroscopes are critical components in various applications, but their performance can be adversely affected by uncertainties and external disturbances. MEMS gyroscopes normally have lots of drawbacks during their works in outside areas like temperature variation, unexpected variation in model parameters as well as the incorrectness in manufacturing errors [3]. To cope with these disadvantages and to enhance the sensitivity and accuracy of micro gyroscopes, the developing of effective controller has become very urgent issue. The existence of these shortcomings will decrease the sensitivity and accuracy of MEMS gyroscopes [4][5].

Various control strategies, including model-based adaptive control [6], back stepping and sliding mode controllers [7]-[14], observer based controllers [15]-[18], fractional order control [19], neural networks and fuzzy control [20]-[25], have been proposed to improve MEMS gyroscope performance. However, many of these methods rely on system dynamics or are computationally intensive.

In spite getting good results from these strategies, it is found they are not sufficient for real time applications this is because of the needing of these methods to include dynamics of system in their formulations [26]. The numerous parameters obtained from using these schemes may greatly weaken the possibility of using them in practical applications [27]. On the other hand, neural networks and fuzzy Control schemes have many drawbacks and disadvantages during their use such as requiring sophisticated training for tuning the parameters of their structures which significantly impact on the overall control performance [28][29]. Hence, neither intelligent nor traditional model-based approaches is proved to be suitable for these complicated applications.

Recently, Time Delay Control (TDC) has been adopted as a useful and successful replacement for the previously described techniques [30]. The structure of Time delay control can be comprised into two main parts: Robust control part and Time Delay Estimation part (TDE) [31]. The core of Time delay control approach is time delay estimation part (TDE). Time delay estimation is a simple but effective approximation approach which has the efficiency of solving mentioned problems in a simple way [32]. The main objective behind choosing TDE as an approximation method is to estimate the lumped unknown dynamics of the system. TDE effectively used the time-delayed values of system states to estimate the present system dynamics, leading to an fascinated model-free structure [33].

The second part of time delay control is the robust control part which is used to improve the overall control performance of various complicated practical applications. Thanks to having these effective and sufficient two parts and its simplicity, TDC structures have been undertaken in various kinds of real time complicated systems, such as overhead cranes [34], wearable exoskeletons [35], quad rotor systems [36], nonlinear systems [37], induction motor [38], biped robot [39].

To ensure an excellent and effective control performance, huge efforts had been made in developing the robust control part of TDC approach. On of attractive robust control methods is Sliding mode control (SMC) method. SMC has lots of fascinated features that made it as the primary choice by scholars and researchers. SMC has the ability to handle the external disturbances and the uncertainties in model parameters of nonlinear dynamic systems. In addition, SMC has low sensitivity to the variations in system's parameter [40]-[42]. Consequently, sliding mode (SM) control and its improved schemes have been proved to be effective schemes to ensure excellent control performance and have been used and applied in TDC schemes for different applications [43]-[48].

Normally, the tuning of robust controller parameters can be carried out using trial-and-error approach. In actual situation, the trial-and-error strategy is vary exhausted and inaccurate. In addition, the incorrect adjusting of these coefficients may lead to reducing the accuracy and efficacy of the developed controller and in some cases may cause to the instability problem [49]. Recently, Meta-heuristic optimization algorithms techniques have adopted as an interesting multi-disciplinary research field [50]. Meta-heuristic techniques have been used as an efficient approach to adjust the coefficients of robust controller in effective manner providing the better performance for the controller [51]. One of the recently developed meta-heuristic algorithms is an Arithmetic Optimization Algorithm (AOA) which has been developed in 2021 [52]. AOA is inspired from main behavior of the arithmetic operators in the mathematics [53]. In the present work, the arithmetic Optimization Algorithm (AOA) has been undertaken to optimize the parameters of proposed controller. Thus, this study introduces a model-free optimal integral sliding mode controller (OTDISMC) that integrates Time Delay Estimation (TDE) with Arithmetic Optimization Algorithm (AOA). Unlike conventional methods, this approach does not depend on system dynamics and provides an efficient means to handle uncertainties. The scheme of proposed controller combines the properties and attributes of an integral sliding mode control that tuned by effective and sufficient optimization algorithm (AOA) and time delay estimation which is undertaken in order to estimate and compensate the lumped unknown system dynamics. To the best of the authors' knowledge, no previous works have been developed to make a combination between TDE scheme and Integral SMC that tuned by AOA for MEMS gyroscope systems. Hence, we can summarize the main points that indicate our contribution in this paper as follows:

(a) Developing a model-free controller combining TDE and integral sliding mode control.

(b) Using AOA for parameter optimization.

(c) Analyzing stability using Lyapunov methods.

(d) Validating the approach through comparative simulations.

This paper is organized as follows: in the second section, the mathematical model of the MEMS gyroscope system is accomplished. The third section is devoted for formulating the scheme of optimal model free controller based on time delay estimation and integral sliding mode surface. The analysis of the stability of the MEMS gyroscope system is carried out in the end of this section. The fourth section is concerned with introducing the procedure work for AOA. The results of computer simulation and the analysis of system performance are explained in section Five. The section six introduces the conclusion and prospective work of this paper.

II. Mathematical Model of MEMS Gyroscope

The mechanical structure for z-axis MEMS gyroscope system has been exhibited in In Fig. 1. It is obvious from figure that springs and dampers have been undertaken for attaching a rigid body with a mass. Two types of modes usually associated with MEMS gyroscope. The first mode is the driving mode whereas the second mode is sensing mode. These two modes of MEMS gyroscope can be taken as a second-order system of spring-mass-damping system [19]. According to this concept, the fundamental coordinates of rotation of MEMS gyroscope axes is formulated. The driving vibration represent the x-axis of MEMS Gyroscope, whereas sensing vibration refer to the direction of y-axis of MEMS gyroscope, the direction of input angular velocity can be represented by the z-axis [21].

The dynamic equations of MEMS gyroscope can be acquired by using the fundamentals of Newton's law [22] [54]. By consideration the influence of errors in the manufacturing of the MEMS gyroscope and considering the linearization process of the dynamical model, the dynamic equations of MEMS gyroscope can be expressed as [24]:

$$\begin{aligned} m\ddot{x} + d_{xx}\dot{x} + d_{xy}\dot{y} + k_{xx}x + k_{xy}y &= u_x + 2m\Omega_z\dot{y} \\ m\ddot{y} + d_{xy}\dot{x} + d_{yy}\dot{y} + k_{xy}x + k_{yy}y &= u_y - 2m\Omega_z\dot{x} \end{aligned} \quad (1)$$

Where: m refer to mass of the block system mass. d_{xx}, d_{yy} stands for the coefficients of damping for X & Y axes respectively. k_{xx}, k_{yy} are the spring coefficients of X & Y axes respectively. k_{xy} represents the coupling coefficient. d_{xy} can be defined as the manufacturing errors parameter u_x, u_y refer to control input signals of X&Y axes respectively. x represent the X-axis coordinate, y is the Y-axis coordinate. Ω_z represent Z-axis angular velocity.

The mathematical model derive in Eq. (1) has dimensional form. this form makes the numerical simulation more difficult and makes the controller design more complex [21]-[25]. In fact, Dimensionless method is very important in simulation of the system and has the ability to realize the simulation easily [55].

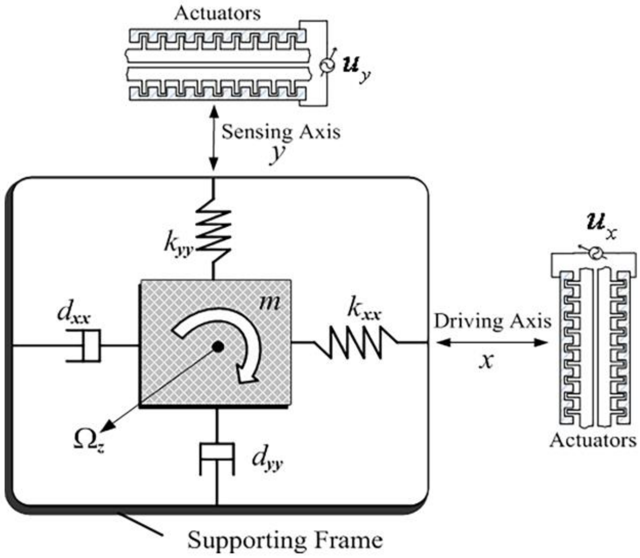

Fig. 1. Schematic structure of a z-axis micro gyroscope [54]

In addition to these properties, dimensionless method provides unified mathematical formula that is used in the design of various types of controllers of MEMS gyroscope systems.

Hence, the using of dimensionless technique has become very urgent to be applied in MEMS gyroscope system model to simply the design of developed controllers [56]. Consequently, the non-dimensional formula of MEMS gyroscope system can be acquired by making the division process on both sides of Eq. (1) by m, q_0 and $\omega_0{}^2$. In fact, m, q_0, and $\omega_0{}^2$ have been considered for converting Eq. (1) into a dimensionless form. q_0 can be defined as the reference length while $\omega_0{}^2$ represent resonance frequency square. According to above, dimensionless form of MEMS gyroscope can be obtained as [55]-[56]:

$$\begin{aligned}\ddot{X} + d_{XX}\dot{X} + d_{XY}\dot{Y} + \omega_X^2 X + \omega_{XY} Y = u_X + 2\Omega_Z \dot{Y}\\ \ddot{Y} + d_{XY}\dot{X} + d_{YY}\dot{Y} + \omega_{XY} X + \omega_Y^2 Y = u_Y - 2\Omega_Z \dot{X}\end{aligned} \quad (2)$$

Where:

$d_{XX} = \frac{d_{xx}}{m\omega_0}$, $d_{XY} = \frac{d_{xy}}{m\omega_0}$, $d_{YY} = \frac{d_{yy}}{m\omega_0}$, $\omega_X^2 = \frac{k_{xx}}{m\omega_0{}^2}$, $\omega_Y^2 = \frac{k_{yy}}{m\omega_0{}^2}$, $\omega_{XY} = \frac{k_{xy}}{m\omega_0{}^2}$, $\Omega_Z = \frac{\Omega_z}{m\omega_0}$

$u_X = \frac{u_x}{m\omega_0{}^2 q_0}$, $u_Y = \frac{u_y}{m\omega_0{}^2 q_0}$.

$X = \frac{x}{q_0}$, $Y = \frac{y}{q_0}$

If we express Eq. (2) in the vector form, following equations can be acquired [24]:

$$\ddot{q} + D\dot{q} + Kq = u - 2\Omega\dot{q} \quad (3)$$

$$\ddot{q} + (D + 2\Omega)\dot{q} + Kq = u + d \quad (4)$$

Where d expresses the unknown external disturbances, and $q = \begin{bmatrix} X \\ Y \end{bmatrix}$, $K = \begin{bmatrix} \omega_X^2 & \omega_{XY} \\ \omega_{XY} & \omega_Y^2 \end{bmatrix}$, $D = \begin{bmatrix} d_{XX} & d_{XY} \\ d_{XY} & d_{YY} \end{bmatrix}$, $u = \begin{bmatrix} u_X \\ u_Y \end{bmatrix}$, $\Omega = \begin{bmatrix} 0 & -\Omega_Z \\ \Omega_Z & 0 \end{bmatrix}$.

III. Model Free Optimal Integral Sliding Mode Control Based on TDE and AOA

In this section, the optimal model-free control law (OTDISMC) based on TDE and ISMC for MEMS gyroscope system is designed to guarantee the error convergence in the presence of parameter variations and outside disturbances. First, we give brief introduction about TDE. Then, an integral sliding mode surface is introduced to develop the controller based on time delay estimation approach. Later, the stability analysis of the system under TDISMC is verified using Lyapunov stability criterion. Finally, to overcome the limitation associated with trial and error method, we introduced the optimized version of the controller (OTDISMC) which depends on Arithmetic Optimization Algorithm (AOA) to tune its parameters.

A. Overview of Time Delay Estimation (TDE)

Time-delay estimation is a famous approach that was developed by Toumi and Ito [57] and Hsia and Gao [58]. The basic concept of Time-delay control includes using time-delayed state variables and control input to estimate the current dynamics of the system in case of having the controller a suitable short sampling period. In spite of the simplicity in its form, TDE scheme is numerically adequate and very resilient [59]. To develop a model free controller based on TDE, the following definition is introduced:

Definition1. [57]. The nonlinear system of function $x(t)$ can be expressed as follows:

$$\dot{x}(t) = f(x,t) + B(x,t)u(t) + d(t) \quad (5)$$

Where: $f(x,t)$ refer to unknown system dynamics, $B(x,t)$ stands for distribution matrix, $d(t)$ represent the unknown external disturbance, and $u(t)$ stands for the control input. By separation between the known and unknown dynamics, Eq. (5) is expressed as follows:

$$f(x,t) + d(t) = \dot{x}(t) - B(x,t)u(t) \quad (6)$$

For performing TDE and obtaining the estimation of unknown dynamics with time delay L, Eq. (6) can be rewritten:

$$\begin{aligned}\hat{f}(x,t) + \hat{d}(\mathrm{t}) &= f(x,t-L) + d(\mathrm{t-L})\\ &= \dot{x}(t-L) - B(x,t-L)u(t-L)\end{aligned} \quad (7)$$

where $\hat{f}(x,t), \hat{d}(\mathrm{t})$ are the estimation of unknown system dynamics.

B. Controller Development

For performing TDE in effective manner, the dynamic equation of a MEMS gyroscope in Eq. (4) can be expressed as [60]:

$$N\ddot{q} + \Psi(q,\dot{q},\ddot{q}) = u \quad (8)$$

Where:

$$\Psi(q,\dot{q},\ddot{q}) = \ddot{q} - N\ddot{q} + (D + 2\Omega)\dot{q} + \mathrm{K}q - d \quad (9)$$

and N is positive constant diagonal matrix which can be invertible whereas $\Psi(q,\dot{q},\ddot{q})$ represent lumped unknown dynamics of MEMS gyroscope (for simplification we will denote $\Psi(q,\dot{q},\ddot{q})$ as Ψ in the remaining of this paper).

Hence, we can formulate the tracking error of the MEMS gyroscope by using Eq. (8) as follows:

$$N\,\ddot{e} + \Psi = u - N\ddot{q}_d \tag{10}$$

$$\ddot{e} = N^{-1}(u - N\ddot{q}_d - \Psi) \tag{11}$$

Where, q and q_d represent the current and desired positions for x & y axes respectively. $\dot{q}$ and $\dot{q}_d$ are the current and desired velocity for x & y axes respectively. $\ddot{q}$ and $\ddot{q}_d$ represent the current and desired acceleration for x&y axes respectively. $\ddot{e} = \ddot{q} - \ddot{q}_d$ refer to the second time derivative of tracking error. In fact, the designing of model-free control using TDE with integral sliding mode controller includes two main parts. The first part includes formulating the efficient sliding surface and the second part is concerned with developing model-free scheme based on TDE. In this paper, an integral sliding surface ISMC is adopted. ISMC offers the benefits of integral skidding surface which has an excellent property of convergence speed. This property gives ISMC the superiority over other schemes of sliding mode manifolds. In this paper, the following sliding surface is undertaken [41]:

$$s = \dot{e} + 2\lambda e + \lambda^2 \int e\,dt \tag{12}$$

Where $e = q - q_d$ is the position error, $\dot{e} = \dot{q} - \dot{q}_d$ refer to the first time derivative of position error, λ is positive vector. The derivative of the selected sliding surface can be determined by using Eq. (11) as follows:

$$\dot{s} = \ddot{e} + 2\lambda\dot{e} + \lambda^2 e = N^{-1}(u - N\ddot{q}_d - \Psi) + 2\lambda\dot{e} + \lambda^2 e \tag{13}$$

In sliding mode controller theory, the control signal usually consists of two main parts: equivalent control part and reaching control law part. The equivalent part can be obtained by setting $\dot{s} = 0$. Whereas reaching control term is added to guarantee the robustness of the system towards unknown dynamics. In this study, the following reaching control part is considered:

$$\dot{s} = -\eta sgn(s) \tag{14}$$

Where η is a constant vector. Thus, the model-free control of the unknown uncertain dynamics of MEMS Gyroscope subjected to unknown external disturbances can be determined to be:

$$u = \Psi + N\ddot{q}_d - 2N\lambda\dot{e} - \lambda^2 Ne - N\,\eta sgn(s) \tag{15}$$

the control performance can be effected because of existing the uncertainties in $\Psi(q,\dot{q},\ddot{q})$. Therefore, $\Psi(q,\dot{q},\ddot{q})$ can be estimated using TDE and using Eq. (5)-(8) as following:

$$\widehat{\Psi} = \Psi_{t-L} = \mathrm{u}_{t-L} - N\,\ddot{q}_{t-L} \tag{16}$$

Where $(t-L)$ denotes a delayed value with a delayed time L. It is obvious from Eq. (16) that for a very small L, $\widehat{\Psi}$ converges to Ψ. The time-delayed acceleration $\ddot{q}_{t-L}$ can be computed by the following approximation [60]:

$$\ddot{q}_{t-L} = \frac{1}{L^2}(q_{\mathrm{t-L}} - 2q_{\mathrm{t-2L}} + q_{\mathrm{t-3L}}) \tag{17}$$

Consequently, the developed model free controller can be acquired by substituting by Ψ in its estimate $\widehat{\Psi}$ in in the control law in Eq. (15) as:

$$u = \widehat{\Psi} + N\ddot{q}_d - 2N\lambda\dot{e} - \lambda^2 Ne - N\,\eta\,sgn(s) \tag{18}$$

Thus, the proposed scheme TDISMC developed in Eq. (18) when applied to the MEMS gyroscope model in Eq. (4), the angular position q tracks the desired trajectory q_{d} appropriately and effectively.

C. Stability Analysis

According to the fundamentals of control system theory, its essential to prove that our developed control has the ability to guarantee robust stability of the MEMS gyroscope system in spite of the existence of model uncertainties and external disturbances. In this work, the analysis of stability of z-axis MEMS gyroscope system developed in Eq. (4) can be verified by using a well-known Lyapunov stability criterion.

Theorem1. If we consider dynamics of the MEMS gyroscope in Eq. (4) with the chosen sliding manifold in Eq. (12), the trajectory of the closed-loop system is converge in a finite time under proposed controller developed in Eq. (18).

Proof. If we take the following Lyapunov function candidate as a candidate function:

$$V(t) = \frac{1}{2}s(t)^T s(t) \tag{19}$$

Taking the first time derivative for Eq. (19), we get:

$$\dot{V}(t) = s(t)^T\dot{s}(t) \tag{20}$$

Substituting Eq. (13) into Eq. (20), one obtains:

$$\dot{V}(t) = s(t)^T\{N^{-1}(u - N\ddot{q}_d - \Psi) + 2\lambda\dot{e} + \lambda^2 e\} \tag{21}$$

Moreover, substituting Eq. (18) into Eq. (21), one has:

$$\begin{aligned}\dot{V}(t) = s(t)^T\{N^{-1}(\widehat{\Psi} + N\ddot{q}_d - 2N\lambda\dot{e} - \lambda^2 Ne \\ - N\,\eta sgn(s) - N\ddot{q}_d - \Psi) + 2\lambda\dot{e} \\ + \lambda^2 e\}\end{aligned} \tag{22}$$

Then, we can get:

$$\dot{V}(t) = s(t)^T\{N^{-1}(\widehat{\Psi} - \eta sgn(s) - \Psi\,\} \tag{23}$$

By simplification of above equation, Eq. (24) can be deduced as:

$$\dot{V}(t) = -\eta\|s\| - N^{-1}\|\xi\|\,\|s\|\,\} \tag{24}$$

Where: $\xi = -(\widehat{\Psi} - \Psi)$ refer to the error obtained after TDE process. This TDE error ξ is bounded with $|\xi_i| \le \sigma_i$ where $\sigma_i > 0, i = 1,2,\ldots..n$.

Because the values of $\eta > 0, N > 0$. The verification of stability of the closed loop system has been accomplished.

Remark 1: One of the common drawbacks associated with sliding mode controller performance is the existence of chattering phenomenon. Therefore, to overcome and eliminate the chattering problem, the sign function in Eq. (14) is replaced by a smooth hyperbolic tangent function which has the following formula [61]-[63]:

$$\tanh(s) = \frac{\mathrm{e}^s - \mathrm{e}^{-s}}{\mathrm{e}^s - \mathrm{e}^{-s}} \tag{25}$$

D. Optimal Integral Sliding Mode Based on Time Delay Estimation (OTDISMC)

The tuning of controller parameters of TDISMC in Eq. (18) (λ, N, η) is normally carried out using trial and error strategy. However, this approach is time consuming and tedious. To handle the drawbacks associated with using trial and error method, a relatively new meta-heuristic optimization technique called Arithmetic Optimization Algorithm (AOA) which introduced in detail in section IV is considered to optimize the coefficients of TDISMC controller. Hence, we obtain OTDISMC controller which has the following formula:

$$u = \hat{\Psi} + N^{*}\ddot{q}_d - 2N^{*}\lambda^{*}\dot{e} - \lambda^{*2}N^{*}e - \eta^{*} N^{*}sgn(s) \quad (26)$$

Where: $(N^{*}, \eta^{*}, \lambda^{*})$, represent optimized values of TDISMC parameters. The block diagram that indicate the methodology of proposed OTDISMC are depicted in Fig. 2.

Remark 2: In Eq. (26), we can observe that the gain matrix N has been multiplied with all items of the developed controller which reflects its significant role in the structure of the controller. Therefore, using trial and error technique in determining the value of N may cause to decreasing the precision. In our study, AOA has been used to assign the values of N matrix. Most of the works developed in past used the trial and error as a method for tuning the matrix N. From this perspective, one of the main aims of the present work is using aan efficient optimization technique to obtain the matrix the values of N matrix appropriately.

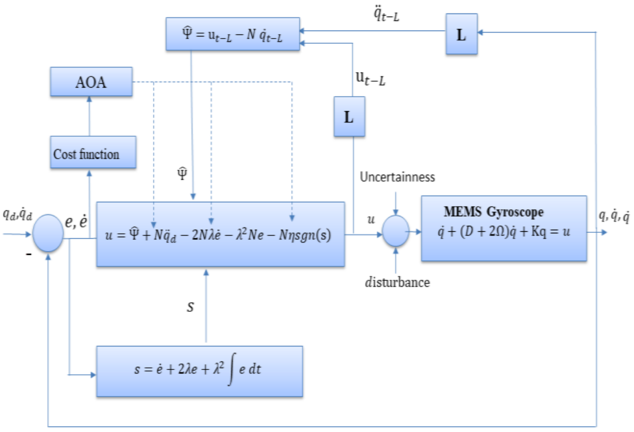

Fig. 2. Block diagram of integral sliding mode controller tuned by AOA algorithm based on Time Delay Estimation

IV. Arithmetic Optimization Algorithm

Arithmetic Optimization Algorithm (AOA) is a population-based meta-heuristic optimization algorithm AOA is mainly inspired from the behavior of the well-known arithmetic operations that are used usually in the mathematics. It is depends on common four operators used in calculations: multiplication (M), division (D), addition (A), and subtraction (S). The first two operators which are the multiplication and division operators are used to explore the search space in exploration phase, whereas exploitation phase include the addition and subtraction operators [64][65].

To distinguish between two phases, math accelerated optimizer MOA function has been used. The expression of MOA function can be written as [66]:

$$MOA(iter) = \text{Min} + \times \left(\frac{Max - Min}{Maxiter}\right) \quad (27)$$

Where: iter refer to the current iterations and maxiter stands for maximum iterations. Min is the minimum value of MOA function and Max represent maximum value of the MOA function [64].

Two phases determined according to the value of MOA. Exploration phase occurs when condition ($r_1 >$ MOA) is verified whereas Exploitation phase occurs when condition ($r_1 <$ MOA) is verified where r_1 is a random generated number. In Exploration phase, the update process can be performed by considering the math operator in the AOA toward the optimum area. Two operation multiplication (M) and the division (D) are mainly divided in Exploration phase. The main objective of this division is to determine the optimal solutions on AOA. In the exploration phase, the positions are updated according to the following formula [64]:

$$x_{i,j}(iter+1) = \begin{cases} best(x_j) \div (MOP + \varepsilon) \times \left((UB_j - LB_j) \times \mu + LB_j\right) \\ \quad r_2 > 0.5 \qquad (a) \\ best(x_j) \times (MOP + \varepsilon) \times \left((UB_j - LB_j) \times \mu + LB_j\right) \\ \quad other\ wise \qquad (b) \end{cases} \quad (28)$$

The jth position of the ith solution at the current position is defined using $x_{i,j}(iter+1)$, while $best(x_j)$ refer to the best solution obtained till now represented by the jth position. ε is a small integer number, UB_j and LB_j denote to the upper bound value and lower bound value of the jth position, respectively. r_2 is a random generated number, μ is a control parameter to adjust the search process. MOP refer to probability math optimizer which can be expressed as [66]:

$$MOP(iter) = 1 - \left(\frac{iter^{1/\alpha}}{maxiter^{1/\alpha}}\right) \quad (29)$$

Where α is a sensitive parameter and defines the exploitation accuracy over the iterations, which is fixed number. The second phase in AOA procedure is an Exploitation phase, The main objective of this phase is to acquire high-dense and optimal solutions. Exploitation phase depends on the work of two main subtraction (S) and the addition (A) operators. The expression that illustrate the work of this phase can be written as [67]:

$$x_{i,j}(iter+1) = \begin{cases} best(x_j) \div (MOP + \varepsilon) \times \left((UB_j - LB_j) \times \mu + LB_j\right) \\ \quad r_3 > 0.5 \qquad (a) \\ best(x_j) \times (MOP + \varepsilon) \times \left((UB_j - LB_j) \times \mu + LB_j\right) \\ \quad other\ wise \qquad (b) \end{cases} \quad (30)$$

r_3 is a random generated number. In this work, we consider an integral time absolute error (ITAE) index as a cost function. ITAE criteria is used for measuring and evaluating positions of AOA. (ITAE) criteria has the following expression:

$$\text{ITAE} = \int_0^T t|e|\,dt \tag{31}$$

The flowchart that explain the procedure work of the AOA is depicted Fig. 3 whereas the position update depending on the AOA algorithm is exhibited in Fig. 4.

To clarify the validity and effectiveness of our proposed control scheme, simulation studies were implemented in Matlab/Simulink. The dynamic model described above will be simulated using MATLAB commands for solving ordinary differential equations. A block diagram of the simulation process is shown in Fig. 5.

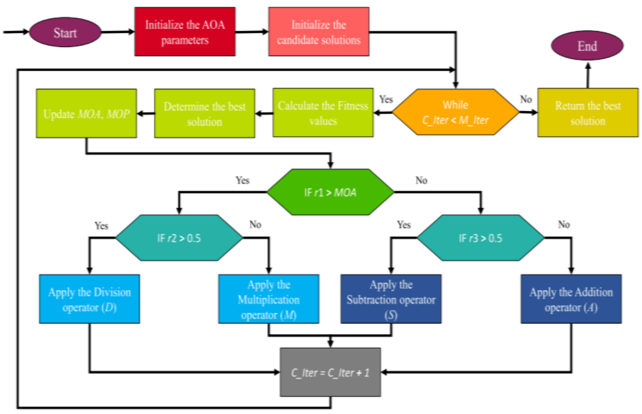

Fig. 3. AOA flowchart [52]

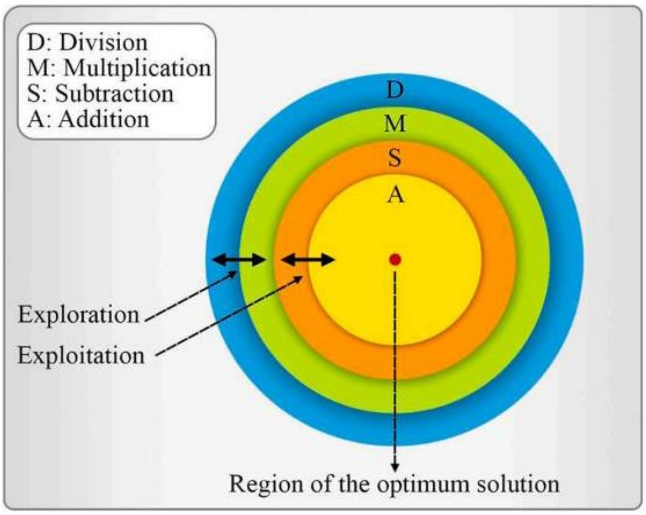

Fig. 4. Position update process for AOA algorithm [64]

V. Results and Discussion

The efficacy of proposed controller (OTDISMC) developed in Eq. (26) is tested by comparing it with TDISMC developed in Eq. (18) that is tuned by trial and error method and the PSO-TDISMC that tuned by PSO algorithm [68][69]. Three tests are conducted to carry out the comparison. The first test is nominal test where the nominal values of MEMS gyroscope system is adopted. The second test is the robustness test where the external disturbance and model uncertainties of MEMS gyroscope parameters have been considered.

The third test is concerned with comparison process between our proposed controller (OTDISMC) and PSO-TDISMC that tuned by PSO algorithm [70].

The values of the adopted MEMS gyroscope have been taken as follows [2][54]:

$m = 1.8 * 10^{-7}\text{k}, k_{xx} = 63.955\,\frac{\text{N}}{\text{m}}, k_{yy} = 95.92\text{N/m}$, $k_{xy} = 12.779\,\frac{\text{N}}{\text{m}}, d_{xx} = 1.8 * \frac{10^{-6}\text{Ns}}{\text{m}}, d_{yy} = 1.8 * 10^{-6}\text{Ns/m}, d_{xy} = 3.6 * 10^{-7}\text{Ns/m}$.

The value of angular velocity of the input is taken as: $\Omega_Z = 100\ \text{rad/sec}$. To simplify the design of the developed controller and implementation for numerical simulation, the dimensionless form for MEMS gyroscope is undertaken. Hence, the value of reference length has been selected as: $q_0 = 1\mu\text{m}$ and reference frequency $\omega_0 = 1000\ \text{Hz}$. Consequently, the values of dimensionless parameters of MEMS gyroscope haven obtained to be:$d_{xx} = 0.01, d_{xy} = 0.002, d_{yy} = 0.01, \omega_x^2 = 355.3,\ \omega_y^2 = 532.9,\ \omega_{XY} = 70.99,\ \Omega_Z = 0.1$.

The desired trajectories of the two axes of MEMS gyroscope have been chosen to be: $q_{d1} = \sin(\pi t)$, $q_{d2} = \cos(\pi t)$. The initial conditions positions and velocities for two axes for both controllers are chosen as: $q_1(0) = 0.2, \dot{q}_1(0) = 1, q_2(0) = 0.5, \dot{q}_2(0) = 1$. The parameter values TDISMC controller which determined by trial and error method have been chosen as: $\lambda = \text{diag}(10,10), \eta = \text{diag}(0.5,0.5\ ), \text{N} = \text{diag}(2,5)$.

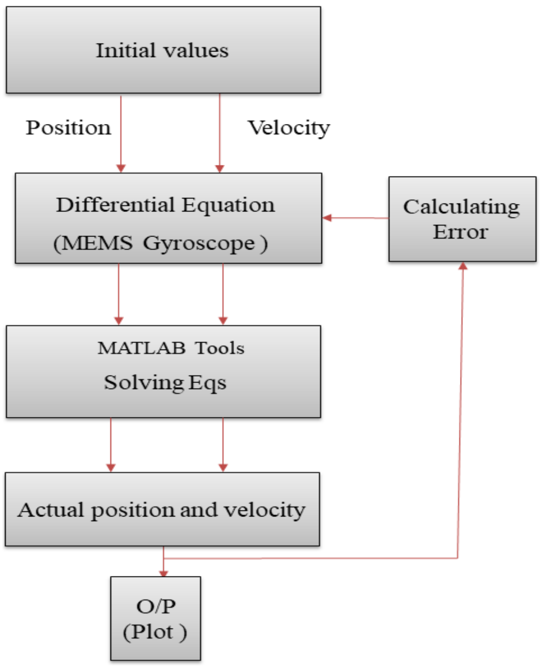

Fig. 5. Block diagram for simulation MEMS gyroscope

The parameter values OTDISMC controller which determined by using AOA algorithm after 120 iterations have been obtained as: $\lambda^* = \text{diag}(13.1,7.9), \eta^* = \text{diag}(0.13,0.42\ ), \text{N}^* = \text{diag}(3.88,6.77)$. The constant time delay has be selected to be L= 0.0001. Parameters values of AOA parameters are indicated in Table I. To investigate the tracking response performance for OTDISMC and TDISMC controllers, an integral absolute value error (IAE) and integrated squared errors (ISE) have been adopted which have the following expressions:

$$IAE = \int |e| \; dt \tag{32}$$

$$ISE = \int |e|^{T} |e| \, dt \tag{33}$$

We can observe the performance of objective function of AOA after 120 iterations in Fig. 6. It is cleared from figure that objective function convergence has been verified after 22 iteration. This indicate the effectiveness and efficiency of this algorithm to tune the coefficients of the developed controller adequately. The evolutions of trajectory tracking position, velocity tracking and position tracking error, in case of nominal values haven been depicted in Figs. 7-9 respectively. It is evident from figures that the two controllers that were synthesized based on time delay control strategy have an excellent tracking performance and good minimizing for the tracking errors. However, OTDISMC controller has the better performance because of the presence of AOA that is used in tuning the controller coefficients. This reflects the vital role of AOA in controller work. It is obvious that the OTDISMC controller can track the desired trajectory for X and Y axes in quick manner. In addition, the smallest values of errors has been acquired using OTDISMC controller as compared with TDISMC controller. If we take Fig.10 to analyze, we can observe that the control input signals for the two controller are very smooth due to the using of integral sliding mode surface and hyperopic tangent function which are able to reduce the chattering effect in adequate manner. Fig. 11 illustrate the convergence of the integral sliding mode surface $s(t)$ for two axes under two control methods. It is noted that the integral sliding surface converge to zero quickly under OTDISMC. The quantitative values of IAE and ISE indices under nominal test are exhibited in Fig. 12 and Fig. 13 and reported in Table II and Table III. The results clearly indicate that OTDISMC has the lowest values of IAE and ISE indices as compared TDISMC controller. The second simulation has been achieved in existence of uncertainties and in the presence of external disturbance. For model uncertainties, the spring and damping coefficients assumed to be changed by ±20% with respect to their nominal values and the coupling terms ω_{XY} and d_{XY} are changed by ±30% [2]. Random signal d = [0.5 rand (1, 1); 0.5rand (1, 1)] has been considered as external disturbance, in fact the using of this value of random signal has been adopted from [25] [54][55]. The results of this test have been depicted in Fig. 14 to Fig. 18. It is observed from these figures that OTDISMC controller have remained excellent and robust against system uncertainty in spite of the existing parameter variations and the presence of external disturbances. Thanks to the depending on TDE, ISMC and AOA in its structure, OTDISMC is still has the best comprehensive control performance, and it is still satisfactory. Moreover, the figures indicate clearly that TDISMC witnessed observable changes in its performance because of using trial and error approach in tuning its parameters. The IAE and ISE indices for the robustness test of two controllers under comparison have been explained in Table IV and Table V and illustrated in Fig. 19 and Fig. 20. It is observed from the quantitative values in Tables IV and Table V that our proposed controller gives lower IAE and ISE values as compared with TDISMC controller. This indicates the efficacy and validity of our developed controller. To be more specific and to sum up, OTDISMC and TDISMC offer excellent tracking of the desired trajectory under uncertainties in model parameters and in the presence of external disturbances. However, OTDISMC can guarantee relatively the best comprehensive control performance.

To further explain the effectiveness our proposed controller of a comparative simulation has been performed between our controller (OTDISMC) and (PSO-TDISMC) that tuned by PSO algorithm. Table VI explain the parameter values for PSO that are used in simulation.

The number of Iterations and population has been chosen as the same as for AOA for fair comparison. The results of this comparison have been explained in Fig. 21 to Fig. 24. It is easy to note the superiority of OTDISMC which tuned by AOA over PSO-TDISMC tuned by PSO. These results indicate the efficacy of AOA algorithm as compared with PSO. The values of IAE and ISE indices of this comparison have been indicated in Fig. 25 and Fig. 26 and Table VII and Table VIII. It is obvious from these indices and tables that OTDISMC outperform PSO-TDISMC in following the desired trajectory and minimization the tracking errors.

In general, the validity of the proposed controller have been proved under two tests. It is conclude that the developed controller ensure excellent tracking performance, eliminate the chattering and has the ability to be robust against model uncertainties and external disturbances.

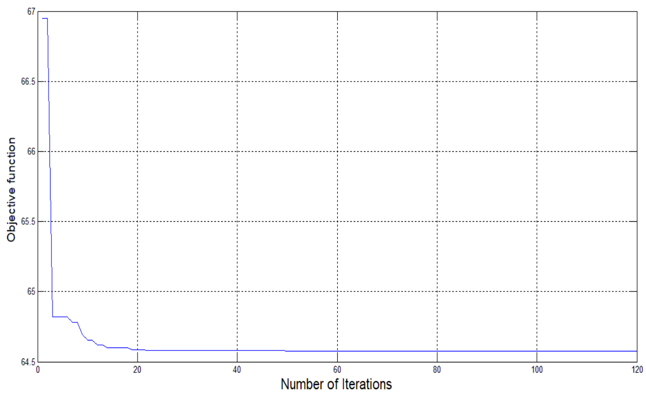

Fig. 6. Evolution of objective function after 120 iterations

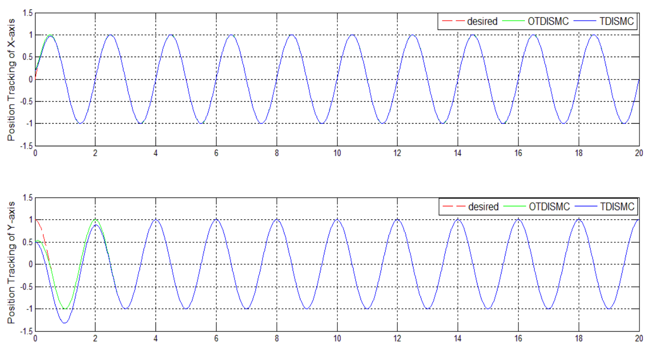

Fig. 7. Trajectory tracking under two controllers for nominal values

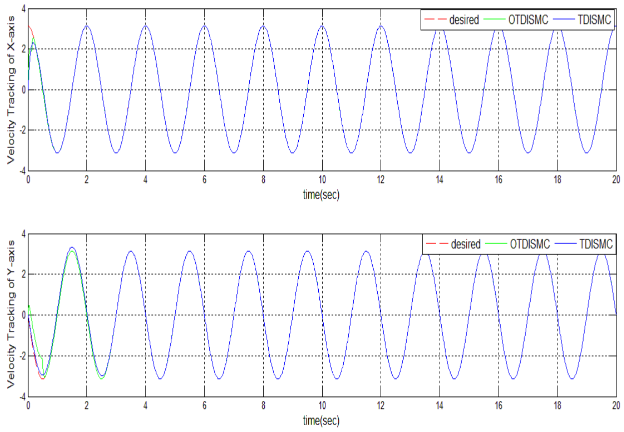

Fig. 8. Velocity of two axes under two controllers for nominal values

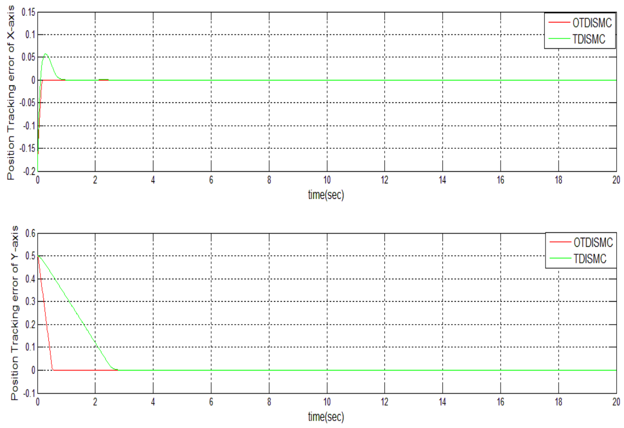

Fig. 9. Trajectory tracking error of two controllers for nominal values

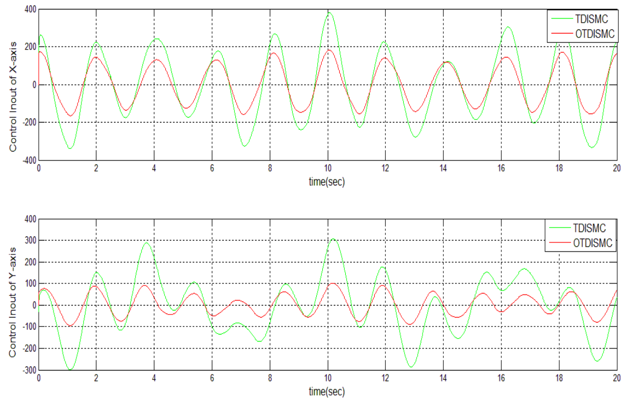

Fig. 10. Control input signals of for two controllers for nominal values

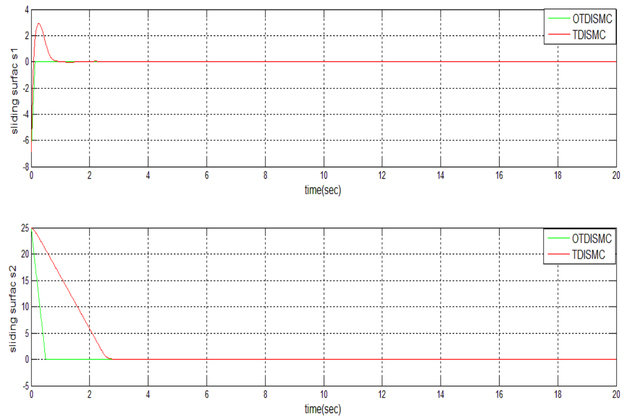

Fig. 11. Sliding surfaces convergence of two controllers for nominal values

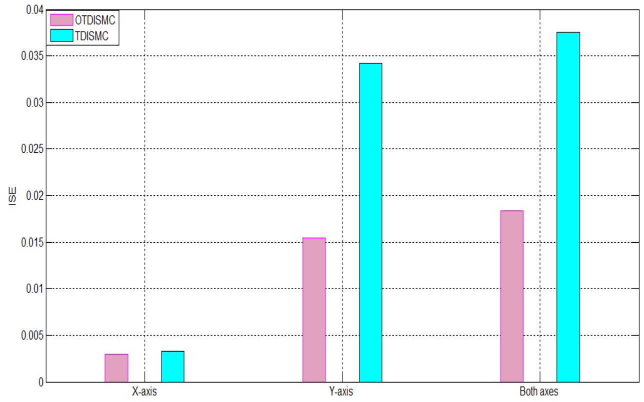

Fig. 12. ISE performance Index for two controllers for nominal values

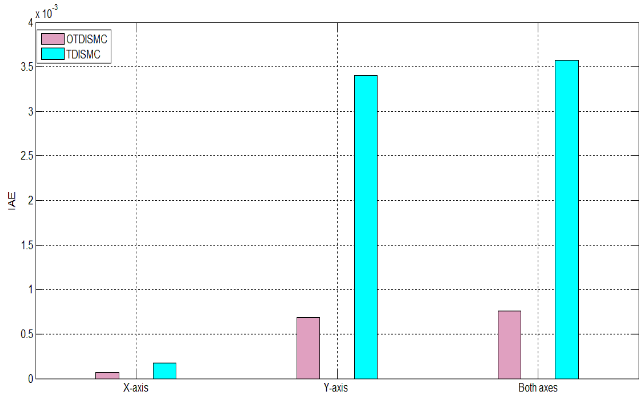

Fig. 13. IAE performance Index for two controllers for nominal values

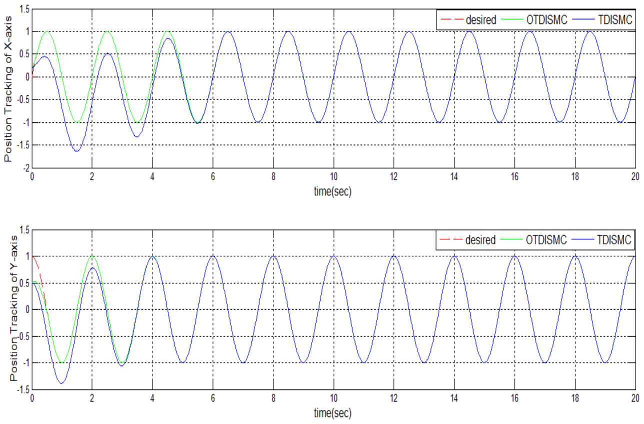

Fig. 14. Trajectory tracking of for two controllers for robustness test

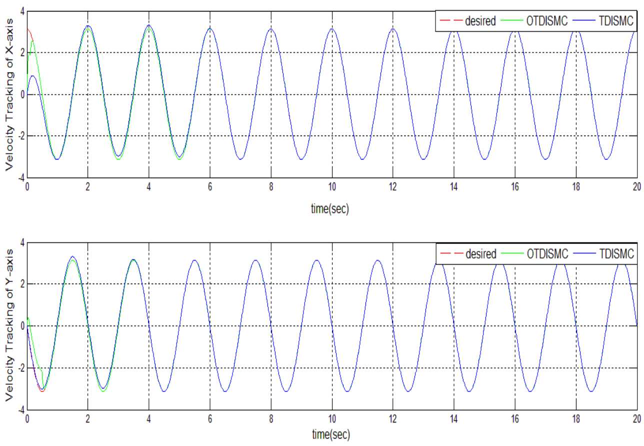

Fig. 15. Velocity of two axes for two controllers for robustness test

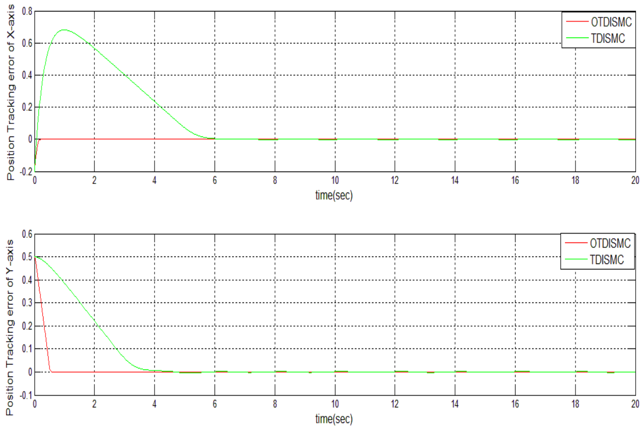

Fig. 16. Trajectory tracking error for two controllers for robustness test

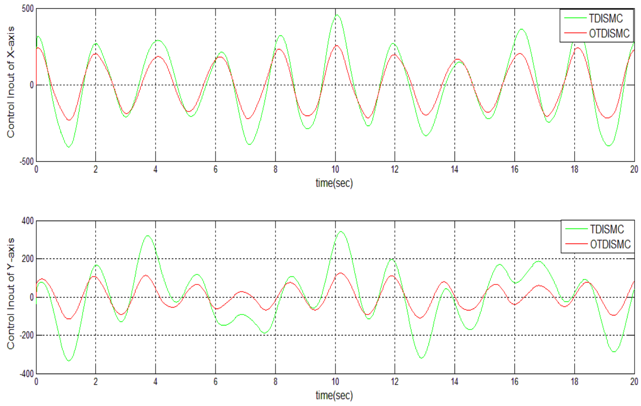

Fig. 17. Control input signals of for two controllers for robustness test

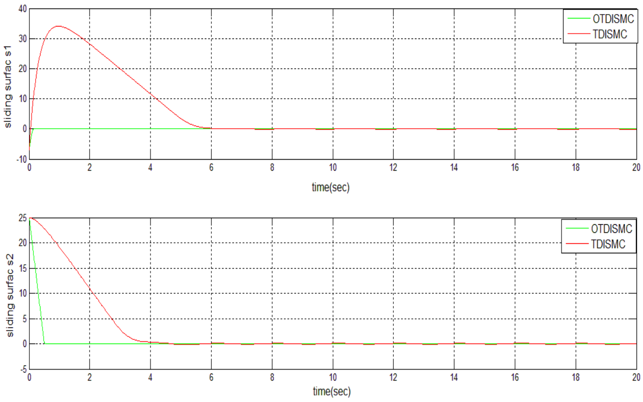

Fig. 18. Sliding surfaces convergence of two controllers for robustness test

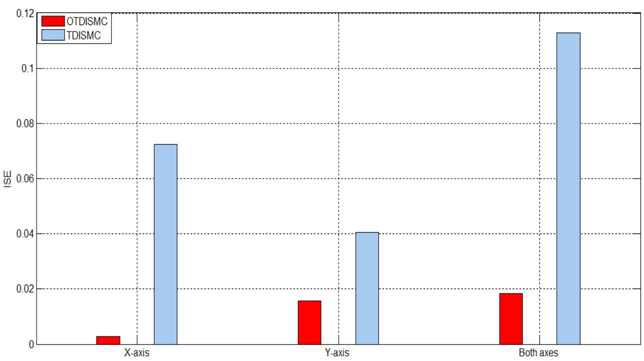

Fig. 19. ISE performance Index for two controllers for robustness test

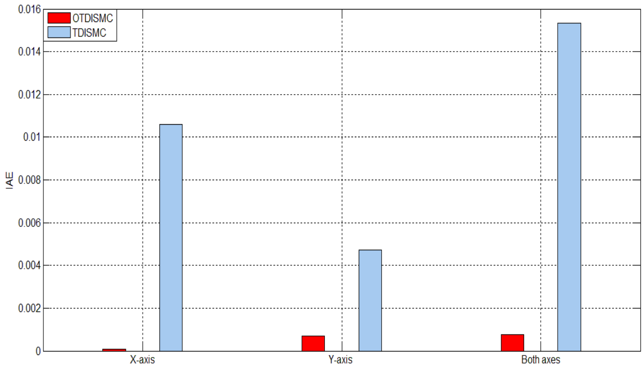

Fig. 20. IAE performance Index for two controllers for robustness test

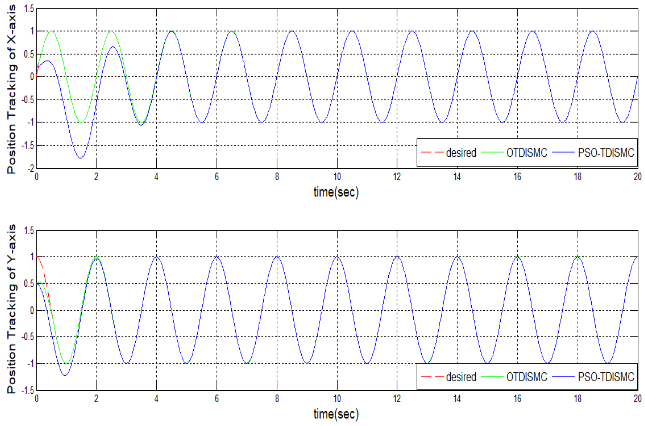

Fig. 21. Trajectory tracking of for two controllers under comparison

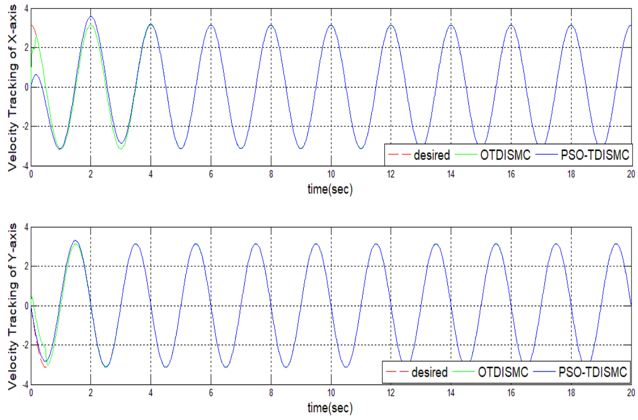

Fig. 22. Velocity of two axes for two controllers under comparison

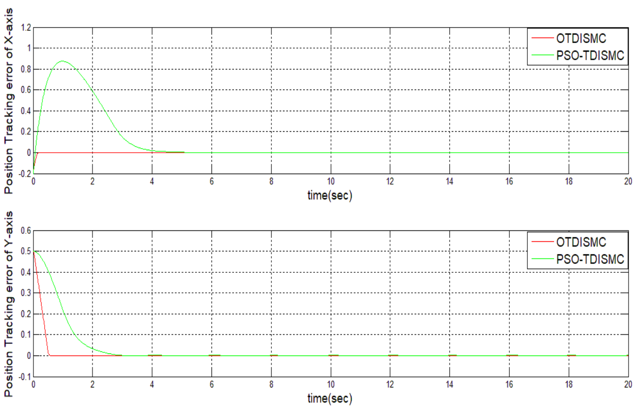

Fig. 23. Trajectory tracking error for two controllers under comparison

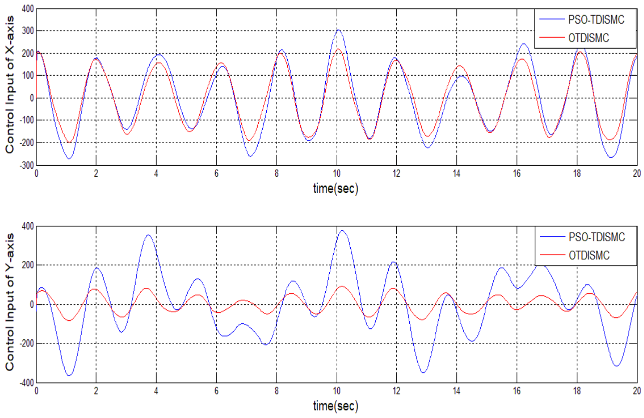

Fig. 24. Control input signals of for two controllers under comparison

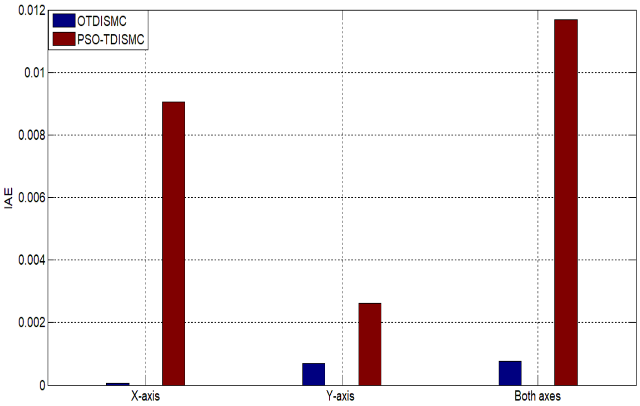

Fig. 25. IAE performance Index for two controllers under comparison

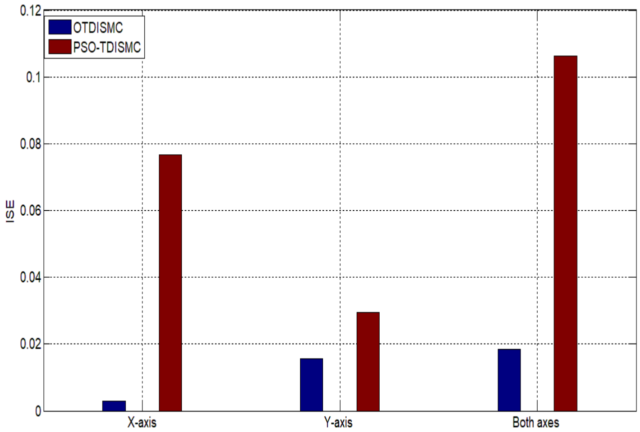

Fig. 26. ISE performance Index for two controllers under comparison

TABLE I. PARAMETERS VALUES FOR AOA

Parameter	Value
Number of Populations	100
Iterations	120
μ	0.5
ε	2
α	5

TABLE II. IAE FOR TWO CONTROLLERS IN NOMINAL TEST

Controllers	axes		
	X-axis	Y-axis	Two axes
OTDISMC	0.0001	0.0007	0.0008
TDISMC	0.0002	0.0034	0.0036

TABLE III. ISE FOR TWO CONTROLLERS IN NOMINAL TEST

Controllers	axes		
	X-axis	Y-axis	Two axes
OTDISMC	0.0030	0.0154	0.0184
TDISMC	0.0033	0.0342	0.0375

TABLE IV. IAE FOR TWO CONTROLLERS FOR ROBUSTNESS TEST

Controllers	axes		
	X-axis	Y-axis	Two axes
OTDISMC	0.0002	0.0007	0.0009
TDISMC	0.0106	0.0047	0.0153

TABLE V. ISE FOR TWO CONTROLLERS FOR ROBUSTNESS TEST

Controllers	axes		
	X-axis	Y-axis	Two axes
OTDISMC	0.0028	0.0156	0.0185
TDISMC	0.0725	0.0404	0.1129

TABLE VI. PARAMETERS VALUES FOR PSO

Parameter	Value
Number of Populations	100
Iterations	120
C_1	2
C_2	2
W	1.6

TABLE VII. IAE FOR CONTROLLERS UNDER COMPARSION

Controllers	axes		
	X-axis	Y-axis	Two axes
OTDISMC	0.0001	0.0007	0.0008
PSO-TDISMC	0.0091	0.0026	0.0117

TABLE VIII. ISE FOR CONTROLLERS UNDER COMPARSION

Controllers	axes		
	X-axis	Y-axis	Two axes
OTDISMC	0.0029	0.0155	0.0184
PSO-TDISMC	0.0767	0.0296	0.1063

VI. CONCLUSION

In this article, a model-free controller based on TDE, ISMC and arithmetic optimization algorithm has been synthesized for controlling of the Z-axis micro gyroscope. The controller has been synthesized by combining the advantages of TDE technique with integral sliding mode surface. The integral sliding mode control enabled the system to acquire excellent control performance, minimum tracking error, smooth control input signals and fast convergence. The lumped unknown dynamics of the MEMS gyroscope has been compensated and estimated by using Time Delay Estimation technique. To overcome the shortcomings associated with using classical trial and error method, AOA has been adopted to adjust the coefficients of developed controller. Stability of closed-loop system has been analyzed based on Lyapunov stability criteria. The proposed controller could be applied in real-world scenarios and has potential impact on industries that use MEMS gyroscopes.

The results of computer simulation clearly indicate the efficacy of the proposed controller by providing excellent trajectory tracking performance, minimizing position and velocities errors and giving smooth control input signals. Additionally, the results proved that developed controller has the ability to be robust in spite of the presence of model uncertainties and unknown external disturbances. The results also demonstrate the validity of the developed controller to compensate the unknown system dynamics for MEMS gyroscope in appropriate manner.

In the future, our objective is developing another scheme time delay based control integrated with higher order sliding mode controller that overcome the possible limitation associated with current controller.

REFERENCE

[1] W. A. Gill, I. Howard, I. Mazhar, and K. McKee, "A review of MEMS vibrating gyroscopes and their reliability issues in harsh environments," *Sensors*, vol. 22, no. 19, p. 7405, 2022.

[2] M. A. Faraj, N. Derbel, and B. Maalej, "Optimal fractional order pd controller for MEMS gyroscope," in *2024 21st International MultiConference on Systems, Signals & Devices (SSD)*, pp. 266–271, 2024.

[3] M. Rahmani, M. H. Rahman, and M. Nosonovsky, "A new hybrid robust control of mems gyroscope," *Microsystem Technologies*, vol. 26, no. 3, pp. 853–860, 2020.

[4] M. Rahmani, "MEMS gyroscope control using a novel compound robust control," *ISA Trans.*, vol. 72, pp. 37–43, Jan. 2017.

[5] Y. Fang, W. Fu, C. An, Z. Yuan, and J. Fei, "Modeling, simulation and dynamic sliding mode control of a MEMS gyroscope," *Micromachines*, vol. 12, no. 2, p. 190, 2021.

[6] H. Wang, L. Hua, Y. Guo, and C. Lu, "Control of z-axis mems gyroscope using adaptive fractional order dynamic sliding mode approach," *IEEE Access*, vol. 7, pp. 133008–133016, 2019.

[7] Y. Fang, J. Fei, and Y. Yang, "Adaptive backstepping design of a micro gyroscope," *Micromachines*, vol. 9, no. 7, p. 338, 2018.

[8] J. Fei and X. Liang, "Adaptive backstepping fuzzy neural network fractional-order control of microgyroscope using a nonsingular terminal sliding mode controller," *Complexity*, pp. 1–12, Sep. 2018.

[9] J. Fei, Y. Fang, and Z. Yuan, "Adaptive fuzzy sliding mode control for a micro gyroscope with backstepping controller," *Micromachines*, vol. 11, no. 11, p. 968, 2020.

[10] S. B. Fazeli Asl and S. S. Moosapour, "Fractional order fuzzy dynamic backstepping sliding mode controller design for triaxial MEMS gyroscope based on high-gain and disturbance observers," *IETE Journal of Research*, vol. 67, no. 6, pp. 799–816, 2021.

[11] L. Zhang, Z. Wen, C. Lu, Y. Guo, X. Zhang, and L. Luo, "Improved fully adjusted neural network based recursive terminal sliding mode control for MEMS gyroscopes," in *2022 5th International Conference on Robotics, Control and Automation Engineering (RCAE)*, pp. 11–16, 2022.

[12] M. Rahmani, M. H. Rahman, and J. Ghommam, "Compound fractional integral terminal sliding mode control and fractional pd control of MEMS gyroscope," *New Trends in Robot Control*, pp. 359–370, 2020.

[13] Y. Guo, B. Xu, and R. Zhang, "Terminal sliding mode control of MEMS gyroscopes with finite-time learning," *IEEE Transactions on Neural Networks and Learning Systems*, vol. 32, no. 10, pp. 4490–4498, 2020.

[14] K. Kant, R. K. Paswan, I. Ahmad, and A. P. Sinha, "Digital control and readout of MEMS gyroscope using second-order sliding mode control," *IEEE Sensors Journal*, vol. 22, no. 21, pp. 20 567–20 574, 2022.

[15] R. Zhang, B. Xu, S. Li, and G. Gao, "Recursive integral terminal sliding mode control with combined extended state observer and adaptive kalman filter for MEMS gyroscopes," *International Journal of Robust and Nonlinear Control*, vol. 34, no. 9, pp. 5706–5718, 2024.

[16] V. Giap, H. Vu, Q. Nguyen, and S.-C. Huang, "Chattering-free sliding mode control-based disturbance observer for mems gyroscope system," *Microsystem Technologies*, vol. 28, no. 8, pp. 1867–1877, 2022.

[17] V. N. Giap, Q. D. Nguyen, N. K. Trung, and S.-C. Huang, "Time-varying disturbance observer based on sliding-mode observer and double phases fixed-time sliding mode control for a ts fuzzy micro-electro-mechanical system gyroscope," *Journal of Vibration and Control*, vol. 29, no.7-8, pp. 1927–1942, 2023.

[18] M. Jafari, S. Mobayen, H. Roth, and F. Bayat, "Nonsingular terminal sliding mode control for micro-electro-mechanical gyroscope based on disturbance observer: Linear matrix inequality approach," *Journal of Vibration and Control*, vol. 28, no. 9-10, pp. 1126–1134, 2022.

[19] M. Rahmani and S. Redkar, "Fractional robust data-driven control of nonlinear MEMS gyroscope," *Nonlinear Dynamics*, vol. 111, no. 21, pp. 19 901–19 910, 2023.

[20] J. Fei and Z. Wang, "Multi-loop recurrent neural network fractional order terminal sliding mode control of MEMS gyroscope," *IEEE Access*, vol. 8, pp. 965–974, 2020.

[21] Y. Fang, W. Fu, H. Ding, and J. Fei, "Modeling and neural sliding mode control of MEMS triaxial gyroscope," *Advances in Mechanical Engineering*, vol. 14, no. 3, 2022.

[22] Z. Wang and J. Fei, "Double loop neural fractional-order terminal sliding mode control of MEMS gyroscope," in *2021 Second International Symposium on Instrumentation, Control, Artificial Intelligence, and Robotics (ICA-SYMP)*, pp. 1–4, 2021.

[23] Z. Feng and J. Fei, "Super-twisting sliding mode control for micro gyroscope based on RBF neural network," *IEEE Access*, pp. 1–13, 2019.

[24] J. Fei and Z. Feng, "Fractional-order finite-time super-twisting sliding mode control of micro gyroscope based on double-loop fuzzy neural network," *IEEE Transactions on Systems, Man, and Cybernetics: Systems*, vol. 51, no. 12, pp. 7692–7706, 2020.

[25] J. Fei and Z. Feng, "Adaptive fuzzy super-twisting sliding mode control for microgyroscope," *Complexity*, vol. 2019, no. 6, pp. 1–13, 2019.

[26] P. Gao, X. Lv, H. Ouyang, L. Mei, and G. Zhang, "A novel model-free intelligent proportional-integral super twisting nonlinear fractional-order sliding mode control of PMSM speed regulation system," *Complexity*, vol. 2020, no. 1, p. 8405453, 2020.

[27] D. Elleuch and T. Damak, "Robust model-free control for robot manipulator under actuator dynamics," *Mathematical Problems in Engineering*, vol. 2020, no. 1, p. 7417314, 2020.

[28] H. Wang, G. I. Mustafa, and Y. Tian, "Model-free fractional-order sliding mode control for an active vehicle suspension system," *Advances in Engineering Software*, vol. 115, pp. 452–461, 2018.

[29] P. Gao, G. Zhang, and X. Lv, "Model-free control using improved smoothing extended state observer and super-twisting nonlinear sliding mode control for pmsm drives," *Energies*, vol. 14, no. 4, p. 922, 2021.

[30] S. Ahmed, A. T. Azar, and I. K. Ibraheem, "Model-free scheme using time delay estimation with fixed-time FSMC for the nonlinear robot dynamics," *AIMS Mathematics*, vol. 9, no. 4, pp. 9989–10009, 2024.

[31] S. Ahmed, H. Wang, and Y. Tian, "Model-free control using time delay estimation and fractional-order nonsingular fast terminal sliding mode for uncertain lower-limb exoskeleton," *Journal of Vibration and Control*, vol. 24, no. 22, pp. 5273–5290, 2018.

[32] A. Rezoug and M. Hamerlain, "Adaptive neural super twisting controller based on terminal sliding mode and time delay estimation method for robotic manipulator," *International Journal of Digital Signals andSmart Systems*, vol. 1, no. 4, pp. 348–364, 2017.

[33] M. Taefi and M. A. Khosravi, "A model free adaptive-robust design for control of robot manipulators: Time delay estimation approach," *International Journal of Robust and Nonlinear Control*, 2024.

[34] S. Liu and W. Xu, "Model-free robust adaptive control of overhead cranes with finite-time convergence based on time-delay control," *Transactions of the Institute of Measurement and Control*, vol. 45, no. 6, pp. 1037–1051, 2023.

[35] J. Sun, J. Wang, P. Yang, and S. Guo, "Fractional-order prescribed performance sliding-mode control with time-delay estimation for wearable exoskeletons," *IEEE Transactions on Industrial Informatics*, vol. 19, no. 7, pp. 8274–8284, 2022.

[36] J. Baek and J. Jung, "A model-free control scheme for attitude stabilization of quadrotor systems," *Electronics*, vol. 9, no. 10, p. 1586, 2020.

[37] H. V. A. Truong, M. H. Nguyen, D. T. Tran, and K. K. Ahn, "A novel adaptive neural network-based time-delayed estimation control

for nonlinear systems subject to disturbances and unknown dynamics," *ISA transactions*, vol. 142, pp. 214–227, 2023.

[38] Y. Kali, M. Ayala, J. Rodas, M. Saad, J. Doval-Gandoy, R. Gregor, and K. Benjelloun, "Time delay estimation based discrete-time supertwisting current control for a six-phase induction motor," *IEEE Transactions on Power Electronics*, vol. 35, no. 11, pp. 12 570–12 580, 2020.

[39] Y. Kali, M. Saad, J. F. Boland, and C. Fallaque, "Walking control using TDE-based Backstepping SM of position-commanded Nao biped robot with matched and unmatched perturbations," *Journal of Control, Automation and Electrical Systems*, vol. 33, no. 6, pp. 1633–1642, 2022.

[40] M. Boukattaya, N. Mezghani, and T. Damak, "Adaptive nonsingular fast terminal sliding-mode control for the tracking problem of uncertain dynamical systems," *ISA transactions*, vol. 77, pp. 1–19, 2018.

[41] F. Massaoudi, D. Elleuch, and T. Damak, "Robust control for a two dof robot manipulator," *Journal of Electrical and Computer Engineering*, vol. 2019, no. 1, p. 3919864, 2019.

[42] M. A. Faraj, B. Maalej, and N. Derbel, "Optimal sliding mode controller for lower limb rehabilitation exoskeleton in constrained environments," *Indonesian Journal of Electrical Engineering and Computer Science*, vol. 30, no. 3, pp. 1458–1469, 2023.

[43] D. Meng, H. Xu, H. Xu, H. Sun, and B. Liang, "Trajectory tracking control for a cable-driven space manipulator using time-delay estimation and nonsingular terminal sliding mode," *Control Engineering Practice*, vol. 139, p. 105649, 2023.

[44] Z. Wen, Y. Guo, L. Zhang, X. Zhang, C. Lu, and L. Luo, "Adaptive sliding mode control for MEMS gyroscopes based on immersion and invariance manifold," in *2023 9th International Conference on Information, Cybernetics, and Computational Social Systems (ICCSS)*, pp.6–11, 2023.

[45] R. Sarkar, S. M. Amrr, J. K. Bhutto, A. S. Saidi, A. Algethami, and A. Banerjee, "Finite time fractional order ISMC with time delay estimation for re-entry phase of RLV with enhanced chattering suppression," *Acta Astronautica*, vol. 202, pp. 130–138, 2023.

[46] J. Hui, "Coordinated discrete-time super-twisting sliding mode controller coupled with time-delay estimator for PWR-based nuclear steam supply system," *Energy*, vol. 301, p. 131536, 2024.

[47] Z. Song, L. Wang, J. Ling, L. Wang, J. Duan, Y. Wang, and B. Chen, "Time-delay control scheme with adaptive fixed-time convergent super twisting fractional-order nonsingular terminal sliding mode for piezoelectric displacement amplifier," *ISA transactions*, vol. 146, pp. 99–113, 2024.

[48] S. Han, H. Wang, and Y. Tian, "Model-free based adaptive nonsingular fast terminal sliding mode control with time-delay estimation fora12DOF multi-functional lower limb exoskeleton," *Advances in Engineering Software*, vol. 119, pp. 38–47, 2018.

[49] M. A. Faraj, B. Maalej, N. Derbel and O. Naifar, "Adaptive fractional order super-twisting sliding mode controller for lower limb rehabilitation exoskeleton in constraint circumstances based on the grey wolf optimization algorithm," *Mathematical Problems in Engineering*, vol. 2023, 2023.

[50] A. Rezoug, J. Iqbal, and M. Tadjine, "Extended grey wolf optimization–based adaptive fast nonsingular terminal sliding mode control of a robotic manipulator," *Proceedings of the Institution of Mechanical Engineers, Part I: Journal of Systems and Control Engineering*, vol. 236, no. 9, pp. 1738–1754, 2022.

[51] M. A. Faraj and A. M. Abbood, "Fractional order PID controller tuned by bat algorithm for robot trajectory control," *Indonesian Journal of Electrical Engineering and Computer Science*, vol. 21, no. 1, pp. 74–83,2021

[52] L. Abualigah, A. Diabat, S. Mirjalili, M. Abd Elaziz, and A. H. Gandomi, "The arithmetic optimization algorithm," *Computer methods in applied mechanics and engineering*, vol. 376, p. 113609, 2021.

[53] M. Issa, "Enhanced arithmetic optimization algorithm for parameter estimation of PID controller," *Arabian Journal for Science and Engineering*, vol. 48, no. 2, pp. 2191–2205, 2023.

[54] Y. Fang, C. An, W. Juan, and J. Fei, "Adaptive h-infinity tracking control for microgyroscope," *Advances in Mechanical Engineering*, vol. 12, no. 6, p. 1687814020927832, 2020.

[55] J. Fei, Z. Wang, and X. Liang, "Robust adaptive fractional fast terminal sliding mode controller for microgyroscope," *Complexity*, vol. 2020, no. 1, p. 8542961, 2020.

[56] J. Xie, J. Fei, and C. An, "Gated recurrent fuzzy neural network slidingmode control of a micro gyroscope," *Mathematics*, vol. 11, no. 3, p. 509, 2023

[57] K. Youcef-Toumi and O. Ito, "A time delay controller for systems with unknown dynamics," *Journal of Dynamic Systems, Measurement, and Control*, vol. 112, p. 133, 1990.

[58] T. C. Hsia and L. Gao, "Robot manipulator control using decentralized linear time-invariant time-delayed joint controllers," in *Proceedings., IEEE International Conference on Robotics and Automation*, pp. 2070–2075, 1990.

[59] S. Ahmed, I. Ghous, and F. Mumtaz, "TDE based model-free control for rigid robotic manipulators under nonlinear friction," *Scientia Iranica*, vol. 31, no. 2, pp. 137–148, 2024.

[60] Y. Kali, M. Saad, K. Benjelloun, and C. Khairallah, "Super-twisting algorithm with time delay estimation for uncertain robot manipulators," *Nonlinear Dynamics*, vol. 93, pp. 557–569, 2018.

[61] M. A. Faraj, B. Maalej, and N. Derbel, "Fractional order based con-trollers for lower limb exoskeleton in contact environments," in *202320th International Multi-Conference on Systems, Signals & Devices (SSD)*, pp. 705–710, 2023.

[62] M. A. Faraj, B. Maalej, and N. Derbel, "Sliding mode control for lowerlimb rehabilitation exoskeleton contacting with floor," in *2023 20th International Multi-Conference on Systems, Signals & Devices (SSD)*, pp. 109–115, 2023.

[63] M. A. Faraj, B. Maalej, and N. Derbel, "Design and analysis of nonsingular terminal super twisting sliding mode controller for lower limb rehabilitation exoskeleton contacting with ground," in *State Estimation and Stabilization of Nonlinear Systems: Theory and Applications*, pp. 367–386, 2023.

[64] E. S. Ghith and F. A. A. Tolba, "Tuning PID controllers based on hybrid arithmetic optimization algorithm and artificial gorilla troop optimization for micro-robotics systems," *IEEE access*, vol. 11, pp. 27138–27154, 2023.

[65] G. Hu, J. Zhong, B. Du, and G. Wei, "An enhanced hybrid arithmetic optimization algorithm for engineering applications," *Computer Methods in Applied Mechanics and Engineering*, vol. 394, p. 114901, 2022.

[66] K. G. Dhal, B. Sasmal, A. Das, S. Ray, and R. Rai, "A comprehensive survey on arithmetic optimization algorithm," *Archives of Computational Methods in Engineering*, vol. 30, no. 5, pp. 3379–3404, 2023.

[67] M. Ahmadipour, M. M. Othman, R. Bo, M. S. Javadi, H. M. Ridha, and M. Alrifaey, "Optimal power flow using a hybridization algorithm of arithmetic optimization and aquila optimizer," *Expert Systems with Applications*, vol. 235, p. 121212, 2024.

[68] A. Znidi, A. S. Nouri, and N. Derbel, "Trajectory Tracking of Lower Limb Exoskeletons using Fractional Order Sliding Mode Control," *2023 IEEE International Workshop on Mechatronic Systems Supervision (IW_MSS)*, pp. 1-6, 2023.

[69] A. Q Al-Dujaili, A. Falah, D. A. Pereira, and I. K. Ibrahim, "Optimal super-twisting sliding mode control design of robot manipulator: design and comparison study," *Int. J. Adv. Robotic Syst*., vol. 17, no. 6, 2020.

[70] A. J. Humaidi and H. M. Badr, "Linear and Nonlinear Active Disturbance Rejection Controllers for single-link flexible joint robot manipulator based on PSO tuner," *J. Eng. Sci. Technol. Rev*., vol. 1, no. 3, pp. 133–8, 2018.